ION BEAM DAMAGE IN CaF_2*

C. R. WIE, T. VREELAND, JR., AND T. A. TOMBRELLO

Divisions of Physics, Mathematics, and Astronomy

and

Engineering and Applied Science

California Institute of Technology, Pasadena, California 91125

ABSTRACT

The change in lattice parameter and the induced damage are studied in single crystal CaF_2 bombarded by a 15 MeV Cl ion beam. The lattice parameter change (strain) and the damage for increasing ion beam dose ($5 \times 10^{12}/cm^2$ to $7 \times 10^{15}/cm^2$) is observed via x-ray rocking curve analysis using a double-crystal diffractometer and x-ray reflection topography. The ion beam energy (range = $\sim 4.5\mu m$ in CaF_2) is such that both the electronic region and the nuclear cascade region of energy loss show up in the diffraction signal. By kinematical x-ray diffraction theory analysis, the progress of strain/damage depth profile with increasing beam dose is shown explicitly. The increase in strain is non-linear with beam dose for the dose range studied. For increasing beam dose, the strain level in the electronic energy loss region is fixed, while that in the nuclear collision loss region increases effectively until that region becomes completely amorphous.

Submitted to Nuclear Instruments and Methods

---

*Supported in part by the National Science Foundation [DMR83-18274].

ONE OF THE BROWN BAG PREPRINT SERIES IN BASIC AND APPLIED SCIENCE

August 1984

1. INTRODUCTION

Irradiation of insulating materials with energetic ions gives rise to chemical (compositional) and structural changes in the latent tracks which can be chemically etched selectively [1]. The structure of individual latent tracks is usually studied using small angle x-ray or neutron scattering [2]. But these small angle scattering techniques give no information on the overall strain and damage of the irradiated region of the material when the tracks overlap heavily at high beam dose. The x-ray rocking curve technique using a double-crystal diffractometer can be used for the measurement of overall strain and damage induced in the irradiated region. This technique has been used to study the strain/damage induced by keV ion implantation [3]. An MeV ion loses most of its energy by electronic excitation and ionization over most of the range and a relatively small energy is deposited in the nuclear cascade collision near the end of the range, while a keV ion used in ion implantation loses its energy predominantly in the nuclear collision cascade. Thus, the strain/damage induced in materials irradiated by MeV ions contains an important component arising from the electronic energy loss which can be very different in the nature of strain/damage production mechanisms and in the production of defects (point and extended) from that arising from the nuclear collision cascade. It is this electronic energy loss which gives rise to the elongated structure of the ion damage track in insulating materials.

Knowledge of the strain/damage produced in various materials bombarded with MeV ion beams is important in understanding material or device behavior under high energy radiation. In this paper, we report the first example of such a study on single crystal CaF_2, irradiated with a 15 MeV Cl ion beam over a wide range of beam doses.

2. EXPERIMENT

A (111) cut of a single crystal CaF_2 ("Harshaw" product) was bombarded with a 15 MeV Cl ion beam to doses from $5 \times 10^{12}/cm^2$ to $7 \times 10^{15}/cm^2$. The irradiation, approximately normal to the surface, was done at room temperature using the tandem accelerator at Caltech. The beam spots were 2mm diameter circles for beam doses from $5 \times 10^{12}/cm^2$ to $2 \times 10^{14}/cm^2$, or 3×3 mm^2 squares for doses from $4 \times 10^{14}/cm^2$ to $7 \times 10^{15}/cm^2$ with approximately homogeneous areal density. Prior to the irradiation the sample was coated with a thin Au-film of about 50 Å thickness to prevent charging of the sample. The Cl ion range in CaF_2 at this energy calculated from the table by Littmark and Ziegler is about 4.5μm [4]. The x-ray diffraction measurement was done using a double-crystal x-ray diffractometer (see fig. 1) with Cu-Kα_1 radiation. Cu-Kα_1 (wavelength = 1.5406 Å) has an absorption length of about 36.5um in CaF_2, which allows Bragg diffraction to occur from the nuclear collision region as well as from the electronic region of the ion range, with very small loss of intensity due to absorption. The (333) reflection of a (111) cut of CaF_2 was observed from the beam spots. The incoming x-ray beam size was adjusted using slits between the first crystal and the irradiated sample so as to fall within the ion beam spot. A step-scan, with step angle typically about .001 degrees and typically 10 sec duration, was made by a computerized drive and data acquisition system. The x-ray rocking curves (reflecting power vs. angle) taken in this way are given in fig. 2. X-ray topographs taken for the asymmetric reflection from (113) planes are shown in fig. 3.

3. MEASUREMENT AND ANALYSIS

The single crystal CaF_2 contained substructure with typical subgrain size of the order of 1mm (fig. 3). By careful alignment of the incident x-ray beam, it was possible to obtain x-ray reflection from only one subgrain.

In fig. 2, only the lower angle side of the substrate Bragg peak is shown because the damage in the crystal gives rise to an increase in the (111) plane d-spacing (positive strain) which corresponds to a Bragg angle shift to lower angles. The maximum strain corresponding to the satellite peak of maximum angular deviation at each beam dose and the main strain corresponding to the satellite peak of maximum intensity as a function of beam dose is given in fig. 4. In this log-log plot, the maximum strain versus dose has approximately two different slopes, a higher slope for doses less than $4 \times 10^{13}/cm^2$ and a lower slope for doses higher than $4 \times 10^{13}/cm^2$. Also, the intensity of the main satellite peak increases with dose up to $4 \times 10^{13}/cm^2$ and decreases with some fluctuation at higher doses. If we attribute this behavior to the saturation or overlap of cylindrical nuclear track regions, the estimated Cl ion track diameter in CaF_2 is about 18 Å. The rocking curves shown in fig. 2 were analyzed using a kinematical x-ray diffraction theory to get quantitative depth distributions of strain and damage [3,5]. In the kinematical x-ray theory analysis, one assumes that the diffracting crystal is composed of thin parallel lamella each with slightly different lattice parameters corresponding to their (uniform) strain levels (fig. 6). The total diffracted electric field amplitude is calculated by superposition of the electric fields diffracted from each lamella using the thin plate approximation, i.e., kinematical x-ray diffraction theory (see ref. 3 or 5), plus the electric field from the substrate. In this approach, one neglects primary and secondary extinction [5] but takes into account normal absorption by each lamella. This approximation is valid if the experimental reflecting power from each layer is less than about 6%. For Cl ion beam irradiated CaF_2, the maximum reflecting power by the strained layers is less than 3%. The damage at high dose which is considered in terms of the average atomic displacement from a perfect lattice site is assumed spherically symmetric, and gives rise to a correction to the structure factor analogous to a Debye-Waller factor. In this approach of analysis, there is some ambiguity in the position of a specific lamella along the ion range. By considering the energy loss (electronic and nuclear) distribution, the efficiency of producing damage by electronic and nuclear energy deposition processes [6], and the total ion range, one can get the best fit to the experimental x-ray rocking curve. The relative positions of the major damage layers was checked using an asymmetric (113) reflection (incident angle of 6.5° to (111) surface). The rocking curve peaks from deep layers decrease in height more than the peaks from near-surface layers due to normal absorption. The stain/damage depth-distribution obtained in this way is shown in fig. 5. In the rocking curves dots and the solid curve represent experimental and calculated reflecting power, respectively. In the strain/damage distribution, the solid curve and dashed curve represent strain (in percent) and average atomic displacement (in angstroms) respectively.

4. DISCUSSION AND CONCLUSION

The irradiation of insulating crystals with MeV ion beam induces strain and damage through the electronic excitation/ionization process nearer the surface and through the nuclear collision process deeper into the bulk near the end of the ion range. The strains induced results in an observable global lattice expansion normal to the surface, and the total expansion can be measured using a Dektak. The strain/damage depth-distribution can be measured using the x-ray rocking curve technique. The data analyzed by means of a kinematical x-ray diffraction theory, shown in fig. 5, give detailed quantitative strain levels and clearly reveal the progression of strain and damage distribution with beam dose. In the case of CaF_2 bombarded by a 15 MeV Cl ion beam, the strain level in the electronic region (near the surface) is not changed by increasing the beam dose. In contrast, the nuclear collision process induces strain and damage which increases with dose and approaches the surface for high dose irradiation. The strain in the electronic region is about 0.115%. At a dose of $4 \times 10^{13}/cm^2$ with constant depth-distribution (fig. 5), and the average atomic displacement in this region is too small to give any observable effect in the reflecting power. At the same dose, the nuclear cascade collision produces a non-uniform depth distribution in strain with maximum of 0.3% and also a small but observable damage. At the dose $4 \times 10^{15}/cm^2$, the wiggles at the higher angular deviation part of the rocking curve disappear and the reflecting power in this part is the same as the background level, which means that the material becomes completly amorphous in the nuclear stopping region, so that strain can no longer be observed in that region by rocking curve analysis. An increase of damage in the nuclear region from the previous dose is shown in the last diagram in fig. 5. Other crystalline insulating materials and compound semiconductors irradiated by various MeV ion beams are currently being studied using the same technique and others (e.g., RBS channeling and electron microscopy).

In summary, the rocking curve technique with a suitable x-ray diffraction theory analysis gives a detailed quantitative strain/damage depth-distribution for insulating materials irradiated by MeV ion beams. The electronic energy deposition process produces a thick layer of constant strain near the surface, while the nuclear collision process produces non-uniform strain and damage until the material becomes completely amorphous. X-ray reflection topography gives information about the lateral uniformity and substructure of the irradiated area.

5. AKCNOWLEDGEMENTS

One of the authors (C. R. Wie) would like to thank V. S. Speriosu for help in the lab when he first started this project. This work was supported in part by the NSF (DMR83-18274).

REFERENCES

[1] R. L. Fleischer, P. B. Price, and R. M. Walker, Nuclear Tracks In Solids, (University of California Press, Berkeley, 1975).

[2] E. Dartyge, T. P. Duraud, Y. Langevin, and M. Maurette, Phys. Rev. 234 (1981) 5231.

D. Albrecht, P. Armbruster, R. Spohr, M. Roth, K. Schaupert, and H. Stuhrmann, Nucl. Instr. & Meth. 230 (1984) 702.

T. A. Tombrello, C. R. Wie, N. Itoh, and T. Nakayama, Phys. Lett. 100A (1984) 42.

T. A. Tombrello, Nucl. Instr. & Meth., B1 (1984) 23.

[3] V. S. Speriosu, J. Appl. Phys. 52 (1981) 6094.

V. S. Speriosu, B. M. Paine, M.-A. Nicolet, and H. L. Glass, Appl. Phys. Lett. 40 (1982) 604.

[4] U. Littmark and J. F. Ziegler, Vol. 6, Range Distributions For Energetic Ions In All Elements (Pergamon Press, 1980).

[5] W. H. Zachariasen, Theory Of X-Ray Diffraction In Crystals (Wiley, New York, 1945).

[6] E. P. EerNise, J. Appl. Phys. 45 (1974) 167.

H. M. Presby and W. L. Brown, Appl. Phys. Lett. 24 (1974) 511.

FIGURE CAPTIONS

Figure 1: Double-crystal x-ray diffractometer.

Figure 2: X-ray rocking curve data taken for symmetric (333) reflection from (111) CaF_2 bombarded with 15 MeV Cl ion beam to different doses. The wiggles at the higher angular deviation disappear at the dose $4 \times 10^{15}/cm^2$ indicating that the damaged region in the nuclear collision cascade becomes completely amorphous.

Figure 3: X-ray reflection topograph showing substructure inside the beam spots. The dark contrast of the front-edge (with respect to the incoming beam) and the white contrast of the back-edge show that the beam spots protrude above the sample surface.

Figure 4: Maximum strain (nuclear collision region) and main strain (near the surface of electronic region) versus ion beam dose.

Figure 5: Kinematical x-ray diffraction theory analysis of rocking curve data. Left: experimental (dots) and calculated (solid curve) reflecting power versus angle. Right: strain (solid curve) and damage (dotted curve) versus depth.

Figure 6: Schematic cross-section of bombarded region showing the parallel laminat structure of strain distribution assumed in kinematical x-ray diffraction theory analysis of rocking curve data.

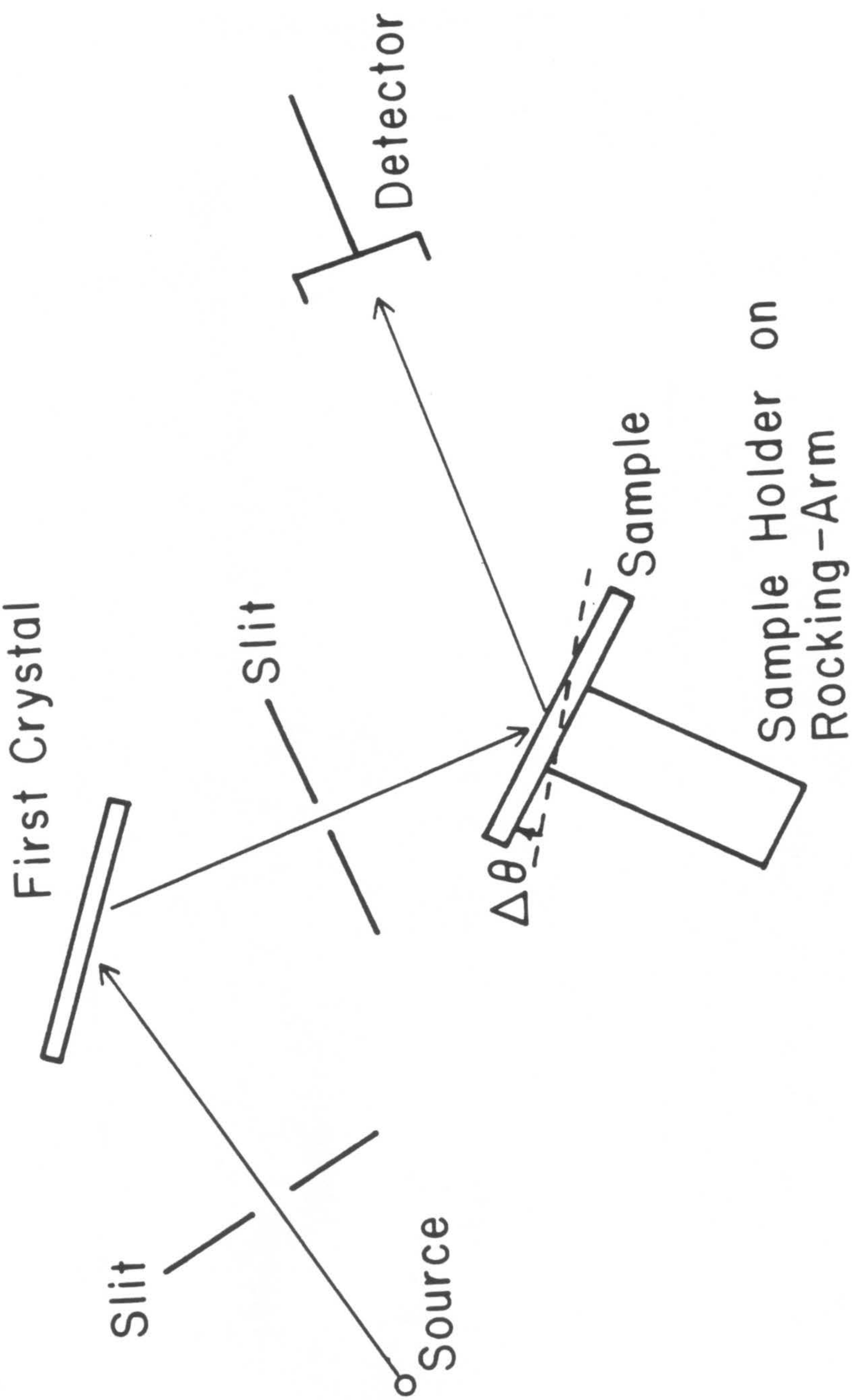

Source
Slit
First Crystal
Slit
Sample
$\Delta\theta$
Sample Holder on Rocking-Arm
Detector

Fig. 1

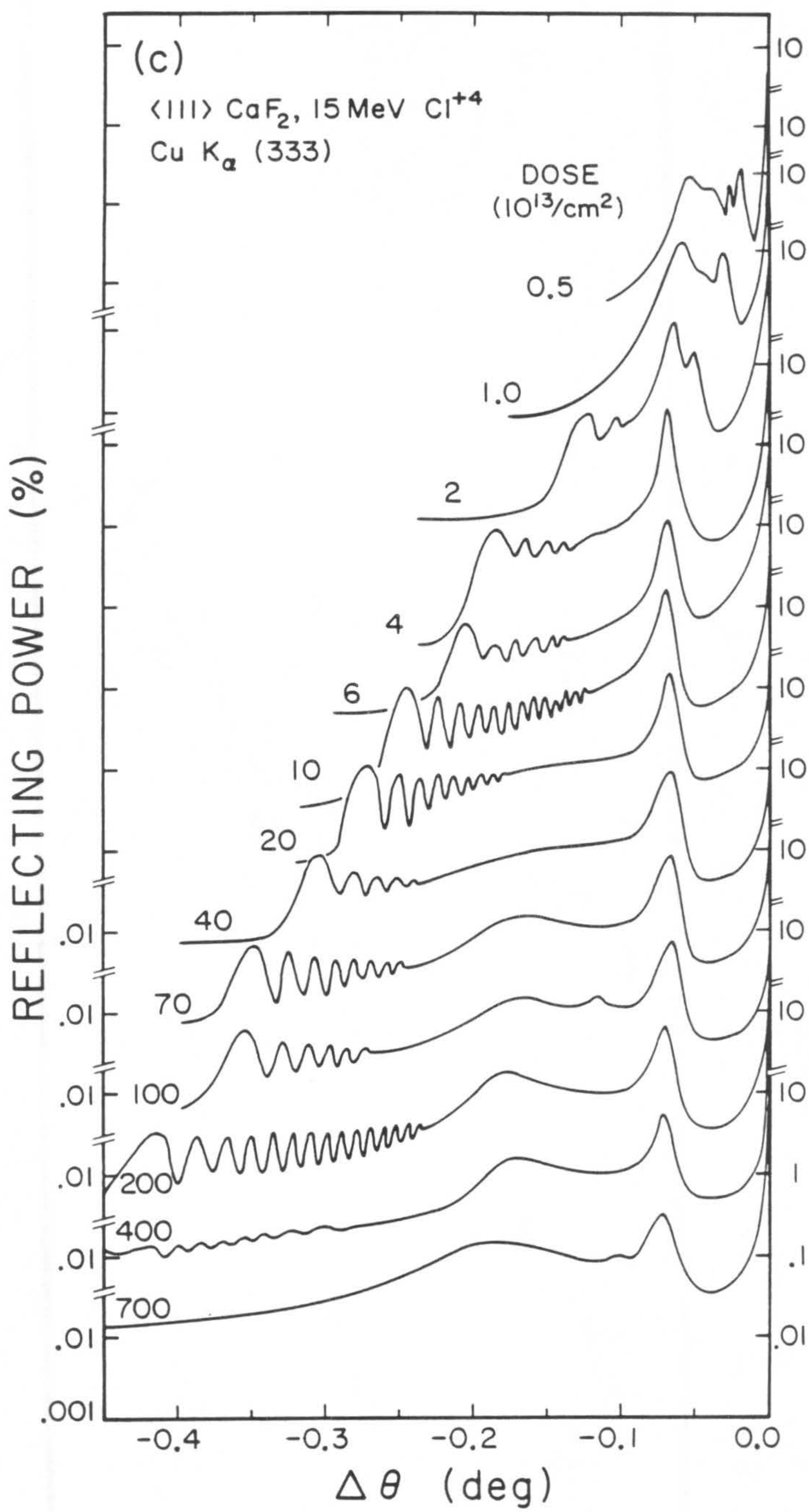
(c)
⟨111⟩ CaF2, 15 MeV Cl+4
Cu Kα (333)
DOSE
(10^13/cm^2)
0.5
1.0
2
4
6
10
20
40
70
100
200
400
700
REFLECTING POWER (%)
Δθ (deg)
-0.4
-0.3
-0.2
-0.1
0.0
.01
.001
10
1
.1

Fig. 2

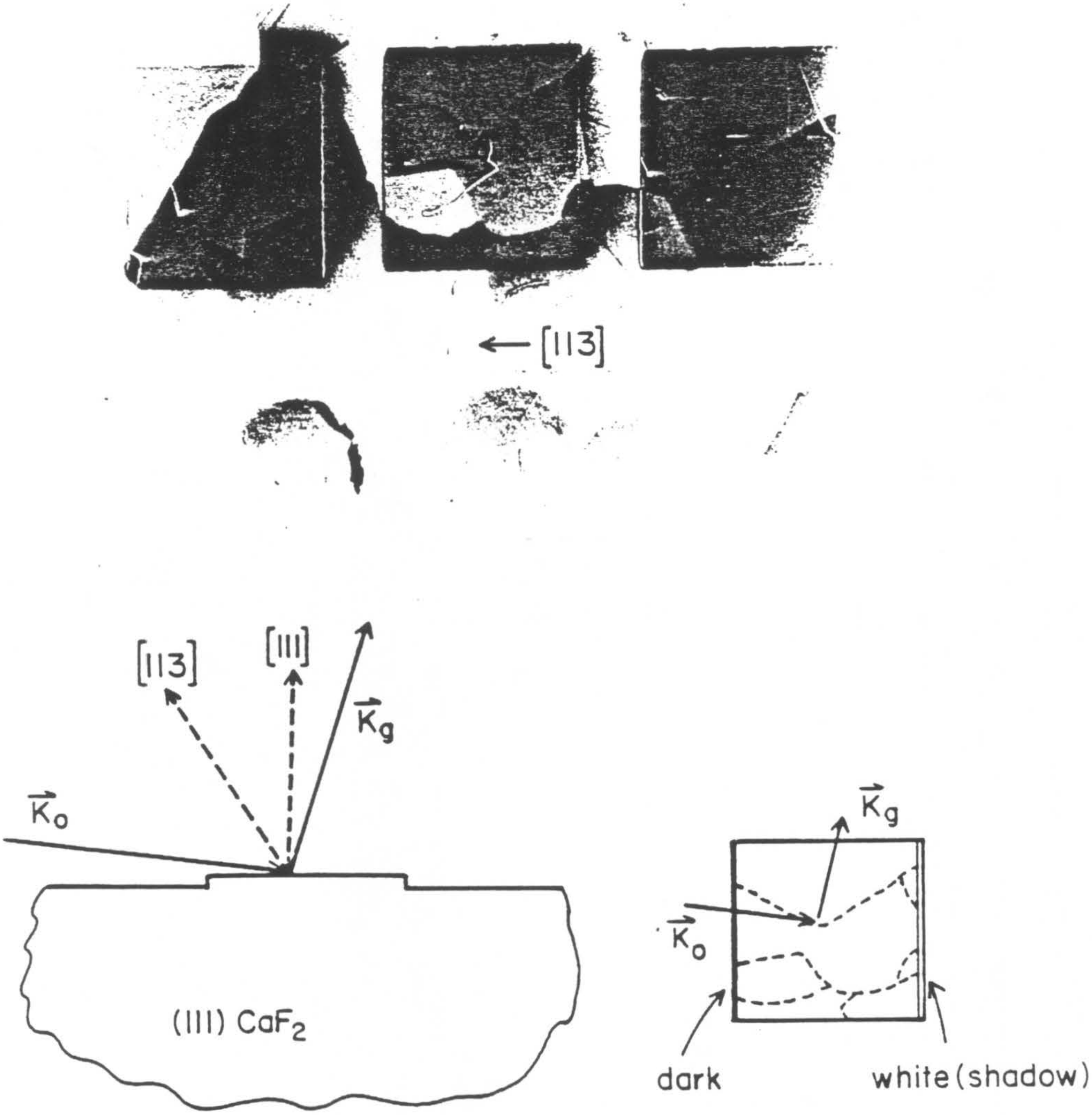
← [113]
[113]
[111]
$\vec{K}_g$
$\vec{K}_o$
(111) CaF_2
$\vec{K}_g$
$\vec{K}_o$
dark
white (shadow)

Fig. 3

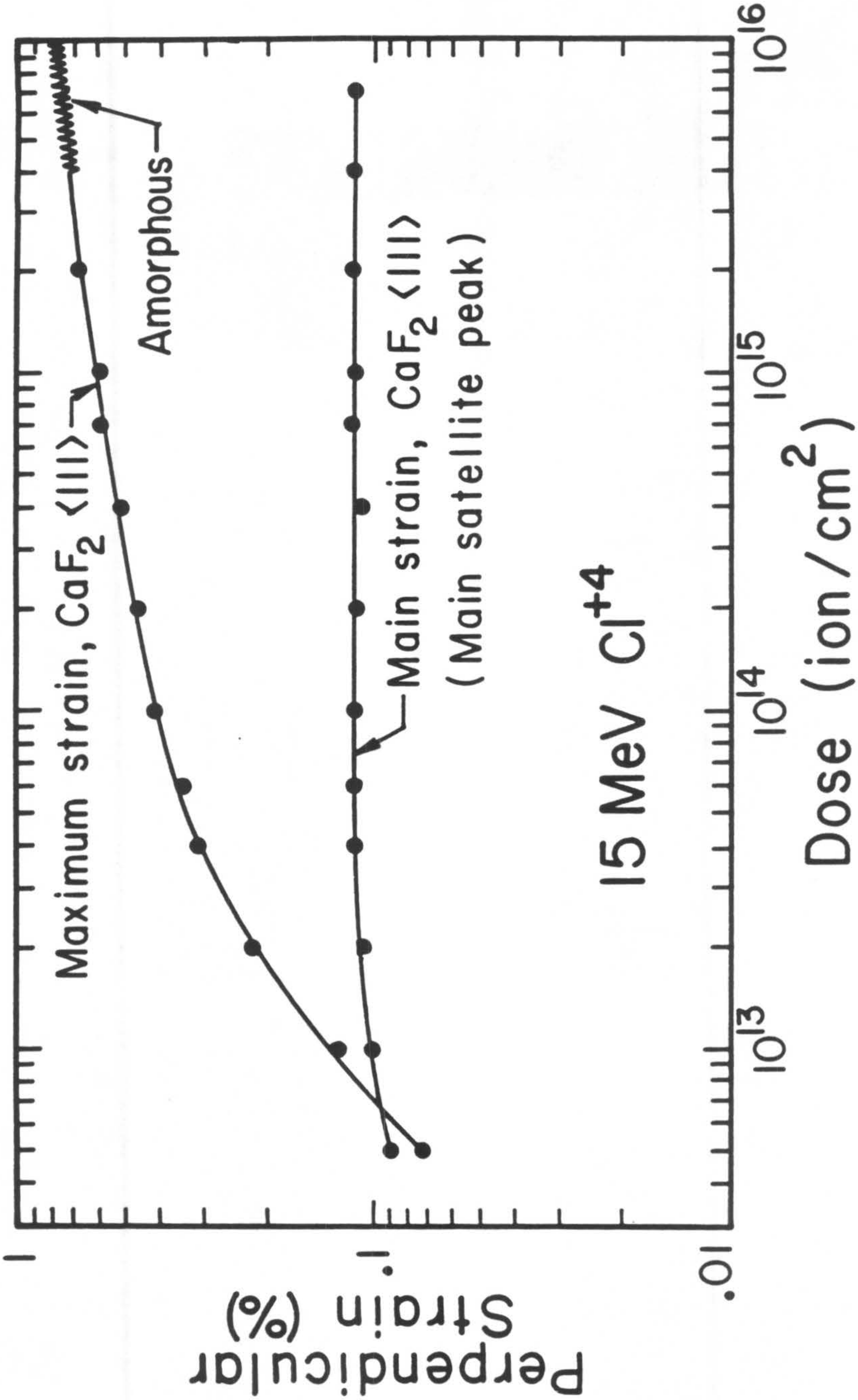
Perpendicular Strain (%)
1
.1
.01
Dose (ion/cm^2)
10^{13}
10^{14}
10^{15}
10^{16}
15 MeV Cl^{+4}
Maximum strain, CaF_2 ⟨111⟩
Amorphous
Main strain, CaF_2 ⟨111⟩
(Main satellite peak)

Fig. 4

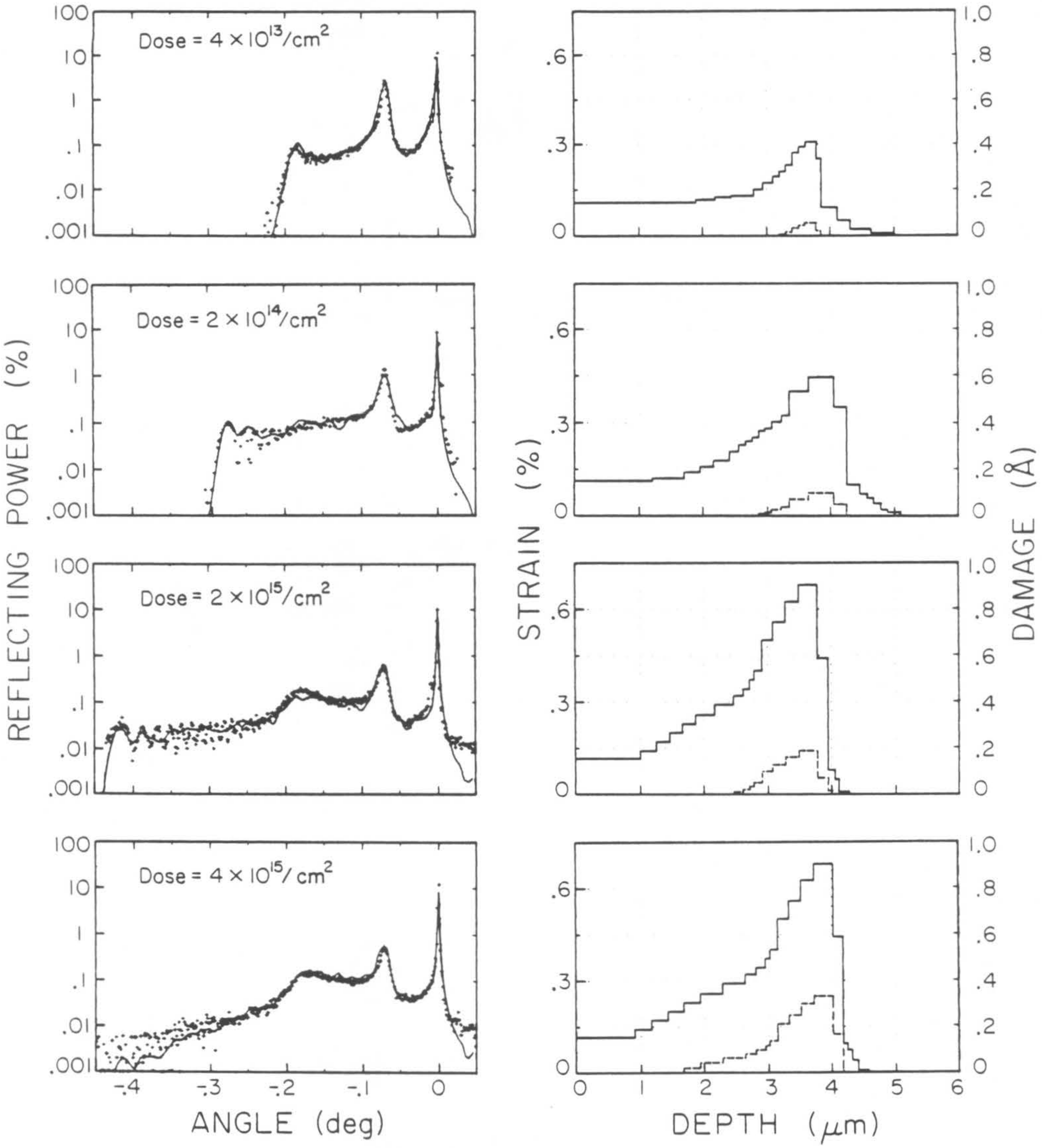
Dose = 4 × 10^13/cm^2
Dose = 2 × 10^14/cm^2
Dose = 2 × 10^15/cm^2
Dose = 4 × 10^15/cm^2
REFLECTING POWER (%)
ANGLE (deg)
STRAIN (%)
DAMAGE (Å)
DEPTH (μm)

Fig. 5

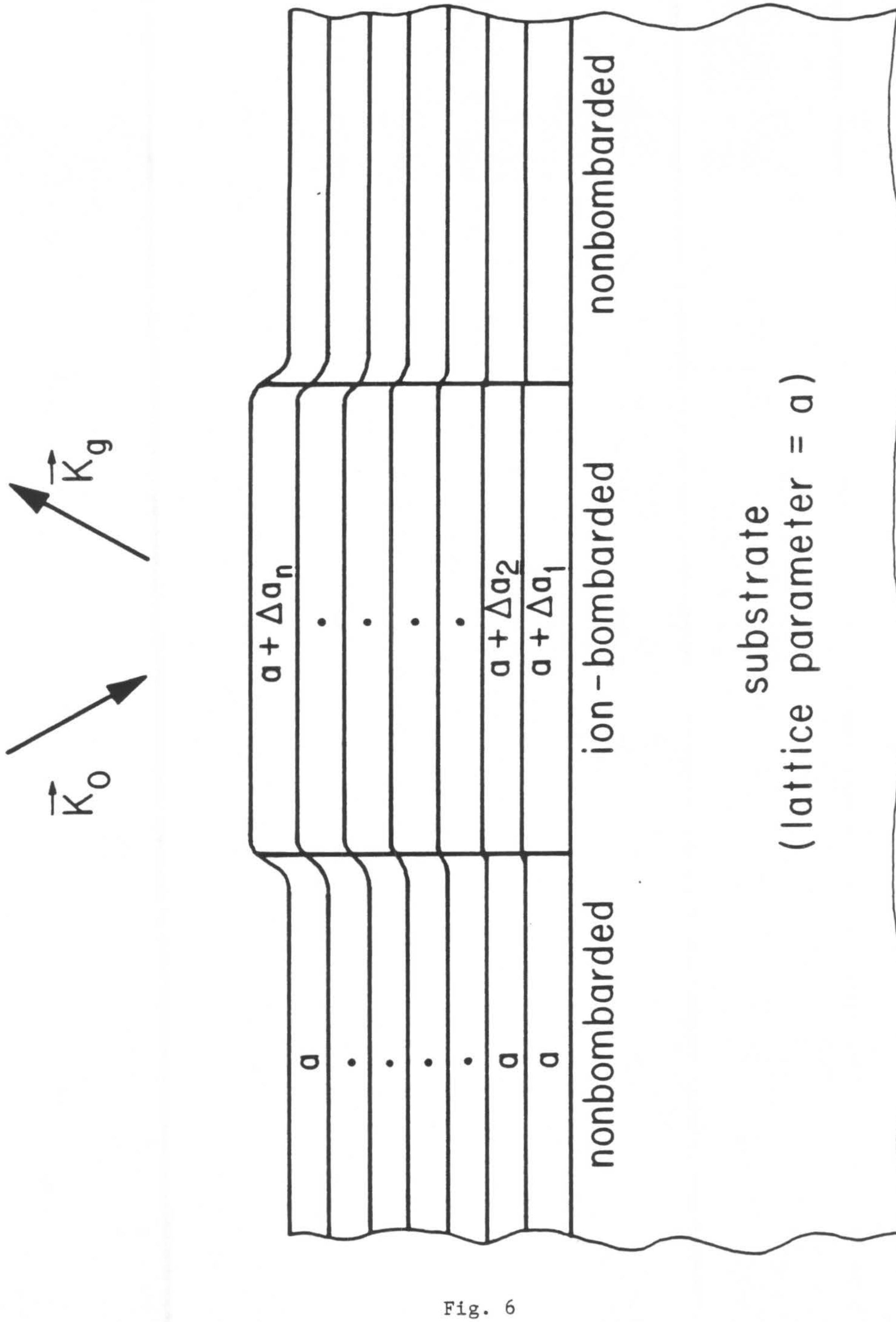

$\vec{K}_0$
$\vec{K}_g$
nonbombarded
ion-bombarded
nonbombarded
$a + \Delta a_n$
$a + \Delta a_2$
$a + \Delta a_1$
a
a
a
substrate
(lattice parameter = a)

Fig. 6